Dielectric dispersion of the relaxor PLZT ceramics in the frequency range 20 Hz-100 THz

2000 J. Phys.: Condens. Matter 12 497

(http://iopscience.iop.org/0953-8984/12/4/309)

J. Phys.: Condens. Matter **12** (2000) 497–519. Printed in the UK PII: S0953-8984(00)05385-6

Dielectric dispersion of the relaxor PLZT ceramics in the frequency range 20 Hz–100 THz

S Kamba†, V Bovtun†, J Petzelt†, I Rychetsky†, R Mizaras‡, A Brilingas‡, J Banys‡, J Grigas‡ and M Kosec§

† Institute of Physics, Academy of Sciences of the Czech Republic, Na Slovance 2, 18221 Praha 8, Czech Republic

‡ Faculty of Physics, University of Vilnius, Sauletekio 9/3, 2040 Vilnius, Lithuania

§ Jozef Stefan Institute, University of Ljubljana, Jamova 39, 1001 Ljubljana, Slovenia

Received 22 June 1999

Abstract. The dielectric dispersion of the transparent relaxor ferroelectric ceramics PLZT 8/65/35 and 9.5/65/35 was determined in a wide frequency range including the microwave and infrared range. The number of observed polar phonons in infrared spectra gives evidence about the locally broken cubic symmetry and the presence of polar nanoclusters in the whole investigated temperature range up to 530 K. A single broad and symmetric dispersion that occurs below the polar phonon frequencies was fitted with the Cole–Cole formula and a uniform distribution of Debye relaxations. On decreasing temperature, the distribution of relaxation times becomes extremely broad which indicates increasing correlation among the clusters. The mean relaxation time diverges according to the Vogel–Fulcher law with the same freezing temperature 230 ± 5 K for both ceramics, but different activation energies 1370 K and 1040 K for the 8/65/35 and 9.5/65/35 sample, respectively. The shortest relaxation time is about 10^{-12} s and remains almost temperature independent. Below room temperature, the loss spectra become essentially frequency independent and the permittivity increases linearly with decreasing logarithm of frequency. The slope of this dependence is proportional to T^4 in the investigated temperature range (above 210 K) which indicates appreciable anharmonicity of the potential for polarization fluctuations.

1. Introduction

Transparent ceramics of lanthanum modified lead zirconate titanate $(Pb_{1-x}La_x)(Zr_yTi_{1-y})O_3$ (PLZT $100(x/y/1-y)$) are extensively studied materials owing to their potential and actual applications in capacitors, actuators, transducers and electro-optic devices since their discovery in 1971 (see the review by Haertling [1]). From the physics point of view attention in the last 15 years was paid especially to relaxor ferroelectric properties [2] characterized by broad frequency-dependent maxima of the temperature-dependent complex dielectric response $\varepsilon^*(T,\omega) = \varepsilon'(T,\omega) + i\varepsilon''(T,\omega)$. The best investigated composition row (close to the morphotropic boundary between the rhombohedral and tetragonal ferroelectric phase where many material coefficients of practical interest show maximal values [1]) is PLZT $x/65/35$ which for $7 < x < 12$ exhibits a typical relaxor behaviour with a very high, broad and dispersive complex permittivity maximum [1, 3]. In this composition range the crystal structure in zero external bias field revealed by x-rays remains simple cubic perovskite ($Pm\bar{3}m$, $Z = 1$) over the whole temperature range [4] and the ferroelectricity can be induced only by a bias field of several kilovolts per centimetre. After switching the field off the polarization remains stable only below a certain temperature called the freezing temperature T_f which is appreciably

0953-8984/00/040497+23$30.00

lower than the temperature of dielectric permittivity and loss maxima T_m [5]. However, clear indications exist that a fluctuating local polarization persists up to much higher temperature corresponding to the ferroelectric transition temperature of pure PZT [6, 7]. This so called Burns temperature is for PLZT $x/65/35$ $T_B \cong 620$ K. Recent TEM experiments [7] suggest that the size of polar nanoregions increases only slightly on cooling below T_B and saturates at about 10 nm below ∼370 K. The diffraction experiment [7] revealed a superlattice reflection which indicates that the local structure of these polar clusters corresponds to the doubled primitive unit cell (rhombohedral space group $R3c$) due to the tilting of oxygen octahedra.

Numerous earlier dielectric studies exist in this series of compositions [1–3, 5, 8, 9]. The activity in this direction continues up to now [10–15], much attention being paid to the problem of freezing, effects of bias field and hysteretic and nonlinear phenomena. Particularly the most recent work by Kutnjak *et al* [15] threw more light upon the complex freezing dynamics in PLZT 9/65/35 and the problem of ergodicity in comparison with other relaxor and dipolar glass systems. However, all the recent dielectric measurements were performed only in the standard low-frequency range of 10–10^6 Hz where only a small part of the very wide dispersion range could be revealed. On the other hand, from the recent infrared (IR) and submillimetre measurements [16–18] it becomes clear that the polar phonon mode contribution to the permittivity in PLZT 8/65/35 and 9.5/65/35 does not exceed 200–300 near room temperature and increases only slightly on heating towards T_B. No phonon softening was observed near the temperature T_m of maximum permittivity, but pronounced dielectric dispersion appeared immediately below the lowest polar phonon frequency. A comparison with the low-frequency permittivity clearly shows that the main dielectric dispersion occurs in the microwave (MW) range practically in the whole temperature range above T_f.

Due to the very high permittivity and loss values, the measurements in the MW range are extremely difficult. In fact, only one measurement up to 10 GHz on a bulk PLZT 8/65/35 sample is known to the authors [8] and recently also a room temperature study on several PLZT thin films has been published [19] which however revealed only a small permittivity not exceeding ∼600 without appreciable dispersion up to 50 GHz. In the mentioned work by Kersten *et al* [8] a single strong polydispersive relaxation was revealed in the GHz range with an Arrhenius-type temperature dependence (above 400 K) of the mean relaxation time. This result differs appreciably from that of later measurements in a more restricted frequency range [9, 10, 13] where a lower relaxation frequency was found, but is not in conflict with the recent measurements by Kutnjak *et al* [15].

The aim of the present work is to obtain and discuss more complete dielectric spectra and their temperature dependences of the best studied relaxor PLZT 8/65/35 and 9.5/65/35 including the MW and IR range on the same material. Recently, we have performed similar measurements on the antiferroelectric PLZT 2/95/5, as well [20]. Our preliminary results on dielectric properties of PLZT 9.5/95/5 [21] and IR properties of PLZT 8/65/35 and 9.5/65/35 [17, 18] have already been published. In section 2, the experimental procedure is briefly described. In section 3, the results are presented and analysed using an approach of uniformly distributed relaxation times above the freezing temperature T_f. Special attention is paid also to the dispersion in the non-ergodic phase below T_f. In section 4, the results are discussed and compared to earlier data and other relaxor materials. In section 5, the main conclusions are drawn.

2. Experiment

The details of the preparation of the PLZT ceramics were already described elsewhere [17]. The dielectric studies were performed by a computer controlled LCR meter HP 4284A in

Table 1. Sample sizes for different frequency bands (r is the radius, d is the length of the cylinder).

PLZT 8/65/35			PLZT 9.5/65/35		
f	r (mm)	d (mm)	f	r (mm)	d (mm)
20 Hz–1 MHz	0.945	0.31	0.1–1 MHz	2.43	0.39
2–50 MHz	0.345	0.285	2–100 MHz	0.51	0.345
50 MHz–4 GHz	0.194	0.82	0.1–1.2 GHz	0.25	0.335
8–12 GHz	0.0834	12	8–12 GHz	0.035	12
above 25 GHz	0.0276	6	above 25 GHz	0.035	6

the frequency range 20 Hz to 1 MHz, by the coaxial (frequency range 1 MHz to 4 GHz) and the waveguide (centimetre and millimetre wave range) dielectric spectrometers [22]. In order to satisfy the conditions of the quasi-stationary microwave electric field distribution in the sample [22], many cylindrical samples have been used to obtain the complete dielectric spectrum. The results presented below were obtained with cylindrical samples of various sizes made for different frequency bands. Sample parameters are listed in table 1.

As the static permittivity of PLZT is rather high and therefore the conditions of the quasi-stationary field distribution in the samples were not satisfied at higher frequencies, the complex permittivity ε^* in decimetre, centimetre and millimetre wave ranges was calculated using equations which take into account the inhomogeneous distribution of the microwave field in the samples [22]. All the measurements were performed in weak electric fields ($E \leqslant 100$ mV cm^{-1}) with a rate of 0.1 K min^{-1} of cooling. It was found that the values of permittivity depend on the phase front related to the thermal gradient and other features in the samples of different dimensions. These features caused scattered points in the figures below.

The IR reflectivity measurements in the spectral range 30–3300 cm^{-1} were carried out using a Bruker IFS113v Fourier transform spectrometer in the temperature interval 10–530 K. Low-temperature measurements were performed using a continuous-flow Oxford CF104 cryostat; high-temperature experiments were done using a simple home-made furnace.

3. Results and analysis

3.1. Dielectric response in the infrared range

Near-normal infrared reflectivity spectra of both PLZT samples are, within the limits of accuracy, the same and do not show any dramatic changes on cooling from 530 K down to 10 K (see figure 1). Infrared reflectivity spectra were taken in the region 30–3300 cm^{-1} (900 GHz–100 THz) but figure 1 shows spectra only below 700 cm^{-1} where all the polar mode reflection bands are present. The reflectivity spectra were fitted with the well known formula [23]

$$R(\omega) \equiv \left| \frac{\sqrt{\varepsilon^*(\omega)} - 1}{\sqrt{\varepsilon^*(\omega)} + 1} \right|^2 \tag{1}$$

and the generalized four-parameter damped oscillator model was used for the complex dielectric function [23]

$$\varepsilon^*(\omega) = \varepsilon'(\omega) + \mathrm{i}\varepsilon''(\omega) = \varepsilon_\infty \prod_j \frac{\omega_{LOj}^2 - \omega^2 + \mathrm{i}\omega\gamma_{LOj}}{\omega_{TOj}^2 - \omega^2 + \mathrm{i}\omega\gamma_{TOj}}. \tag{2}$$

Here ε_∞ is the high-frequency optical permittivity, ω_{TOj} and ω_{LOj} denote transverse and longitudinal eigenfrequencies of the jth polar mode and γ_{TOj} and γ_{LOj} denote their respective

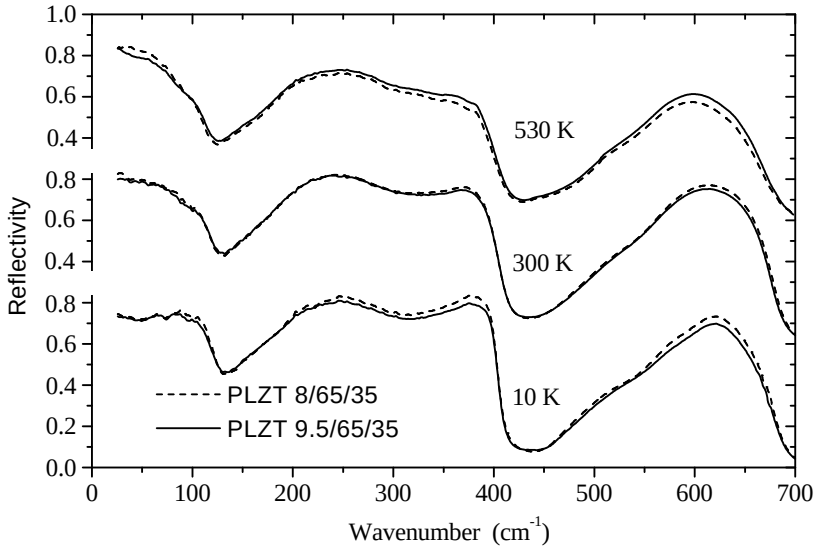

Figure 1. IR reflectivity spectra of PLZT 8/65/35 and 9.5/65/35 at 10, 300 and 530 K.

damping constants. The resulting $\varepsilon'(\omega)$ and $\varepsilon''(\omega)$ spectra are shown in figure 2. The fitted mode parameters for the external and room temperatures are listed in table 2. One can see from figure 2 and table 2 that the phonon contribution to permittivity ε' increases on heating from 110 at 10 K up to 480 at 530 K and lowest-frequency phonon shows remarkable softening. Its frequency ω_s obeys the Cochran law $\omega_s^2 = A(T_B - T)$ with the extrapolated temperature $T_B = 600 \pm 20$ K. Within the accuracy limits, this temperature corresponds to the Burns temperature, below which the polar nanoclusters are supposed to appear.

3.2. Complex dielectric response in the 20 Hz–36 GHz range

The temperature dependences of the real (ε') and imaginary (ε'') parts of the dielectric permittivity at different frequencies for PLZT 8/65/35 are shown in figure 3. Several points are worth mentioning:

(i) Static permittivity of this ceramic is very high: the peak value reaches 12 000 at frequency 0.1 kHz.

(ii) The present results show a typical relaxor behaviour in a very wide frequency range, from low frequencies to millimetre waves, and the peaks of ε' and ε'' move towards higher temperatures with increasing frequency.

(iii) Permittivity remains of the order of 1000 even in the millimetre wave range and losses are also very high ($\tan\delta \geqslant 1$) at MW. This indicates that the main dielectric dispersion occurs in the MW range. The frequency dependence of the real and imaginary part of permittivity at different temperatures is given in figure 4 (room-temperature infrared dielectric response is also included) and shows a typical relaxational dispersion. Near T_m the dispersion begins in the kilohertz region, but at higher temperatures the dispersion occurs in the higher frequency range of 10^7 to 10^{11} Hz as in most order–disorder ferroelectrics [22]. The broad distribution of the relaxation times is seen from the Cole–Cole plot (figure 5). It becomes narrower on increasing temperature.

Table 2. Mode parameters obtained from the fit of reflectivity spectra of PLZT 8/65/35. All mode parameters are expressed in cm^{-1}.

	ω_{TO}			γ_{TO}			ω_{LO}			γ_{LO}			$\Delta\varepsilon$		
No	10 K	300 K	530 K	10 K	300 K	530 K	10 K	300 K	530 K	10 K	300 K	530 K	10 K	300 K	530 K
1	74.9			41			75.2			10			9.9		
2	77	52	28	13	57	48	96	97	91	11	25	31	63.8	176.1	461.1
3	98	99	96	12	22	30	127	122	117	30	35	32	2.2	1.6	2.0
4	203	203	211	47	37	63	326	329	333	79	117	136	22.2	20.8	16.2
5	339	345	357	62	85	109	412	413	412	15	29	33	0.6	0.7	0.7
6	538	529	520	100	84	50	602	569	525	100	93	52	2.3	1.9	0.3
7	589	570	559	67	57	56	683	682	680	22	19	45	0.3	0.1	1.4

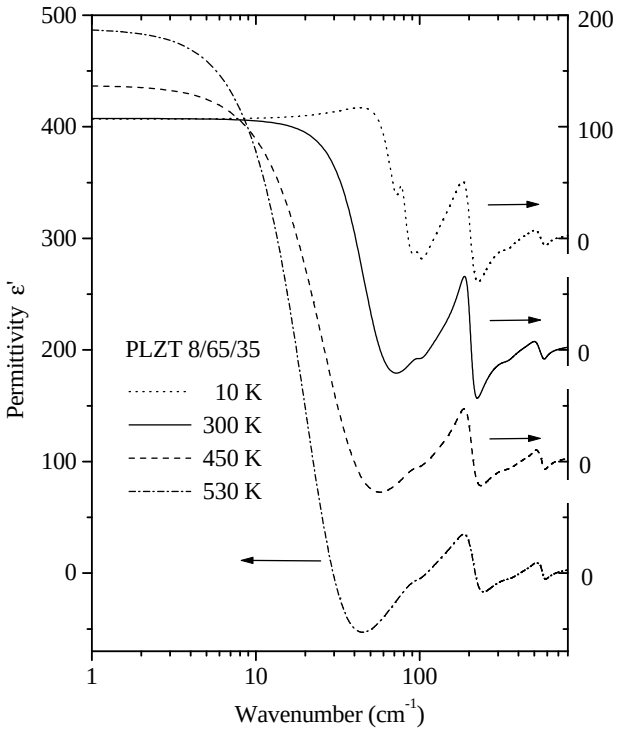

(a)

Figure 2. Real (a) and imaginary (b) part of dielectric function of PLZT 8/65/35 obtained from the fit of IR reflectivity. MW relaxation is not included in the fit. Notice the softening of the lowest-frequency phonon.

Properties of the PLZT 9.5/65/35 ceramics are rather similar to the previous one. Figure 6 shows temperature dependences of the complex permittivity in the frequency range from 100 Hz up to 36 GHz. Both permittivity and losses of this ceramic are smaller than of the previous one. However, both of them exhibit similar temperature and frequency dependences with extremely broad maxima of complex permittivity. The peaks of $\varepsilon'(T)$ and $\varepsilon''(T)$ in PLZT 9.5/65/35 are shifted $\sim$50 K to lower temperatures than in the previous one. Again, at higher temperatures the main dielectric dispersion occurs in the MW range (figure 7). The characteristic Cole–Cole plot (figure 8) shows a broad distribution of the relaxation times.

At low temperatures (below 300 K for PLZT 9.5/65/35), ε'' is almost frequency independent, the dielectric spectrum is very diffuse and a very wide distribution of relaxation times is observed. The frequency independence of ε'' does not allow us to estimate the relaxation time using conventional relaxation models or empirical equations. Therefore the low-temperature dielectric spectra of PLZT 9.5/65/35 will be analysed separately.

3.3. Analysis of the high-temperature dielectric spectra

3.3.1. Empirical Cole–Cole approach. Owing to the roughly symmetrical shape of the Cole–Cole plots at high temperatures (see figures 5 and 8), the diffused dielectric spectra of PLZT

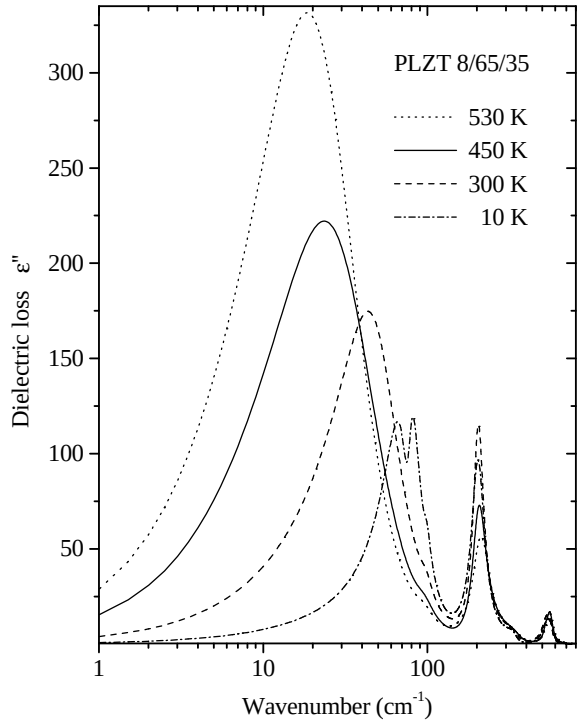

(b)

Figure 2. (Continued)

8/65/35 and PLZT 9.5/65/35 can be fitted by the empirical Cole–Cole equation [22, 24, 25]:

$$\varepsilon^*(\omega) = \varepsilon_\infty + \frac{\Delta\varepsilon}{1 + (\mathrm{i}\omega\tau_0)^{1-\alpha}} \tag{3}$$

where $\Delta\varepsilon = \varepsilon_s - \varepsilon_\infty$ is the contribution of the relaxation to the static permittivity ε_s (dielectric strength), ε_∞ is the contribution of the phonon modes and higher-frequency electronic processes to permittivity, $\omega = 2\pi f$ is the angular frequency and τ_0 is the mean relaxation time. The parameter $0 \leqslant \alpha \leqslant 1$ characterizes the distribution of relaxation times.

We have fitted the experimental Cole–Cole plots at different temperatures with equation (3) and determined the fitting parameters ε_∞, $\Delta\varepsilon$, τ_0 and α. The almost temperature independent value $\varepsilon_\infty \approx 200$ corresponds well to the contribution of phonon modes from IR spectra (see figure 2). Temperature dependences of the fitted parameters τ_0 and α are shown in figure 9. The continuous lines in figures 4, 5, 7 and 8 are fits with the parameters shown in figure 9. Cole–Cole fits were performed only in the limited temperature interval where the fits are reliable. At high temperatures, the relaxation frequencies approach the phonon soft mode which is above the investigated frequency range.

The rapid increase in the mean relaxation time τ_0 with the temperature decrease (about 1000-fold in the interval of 100 K—see figure 9) shows a substantial slowing down of the relaxation processes. The simultaneous increase in the distribution parameter α up to the value of about 0.8 shows that the dielectric spectrum becomes extremely diffuse. Correspondingly, the distribution of the relaxation times becomes extremely wide. It can be estimated using one of the models for the distribution function of the relaxation times.

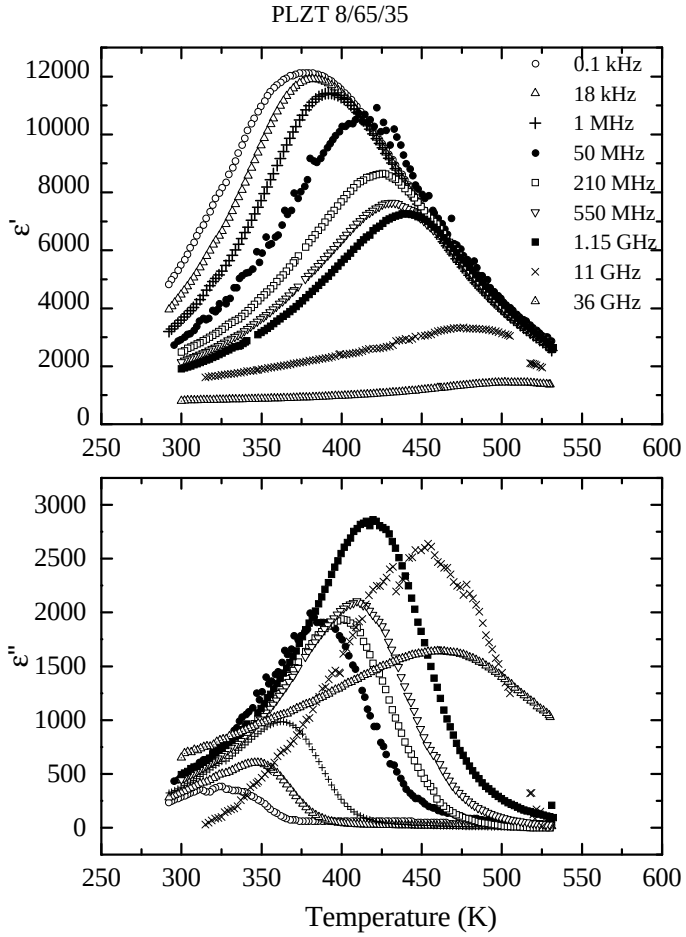

Figure 3. Temperature dependence of the real (ε') and imaginary (ε'') part of complex permittivity of PLZT 8/65/35 at various frequencies.

3.3.2. Approach of the uniform distribution function of the relaxation times. According to the Debye theory, the diffused relaxational dielectric spectrum can be described by means of the distribution function of the relaxation times $g(\tau)$ [24, 25]:

$$\varepsilon^*(\omega) = \varepsilon_\infty + \int_0^\infty \frac{g(\tau)}{1 + \mathrm{i}\omega\tau}\,\mathrm{d}(\ln\tau) \tag{4}$$

where $g(\tau)$ is normalized by the total dielectric strength:

$$\Delta\varepsilon = \int_0^\infty g(\tau)\,\mathrm{d}(\ln\tau). \tag{5}$$

In our next discussion let us assume that $g(\tau)$ is uniform. The uniform $g(\tau)$ corresponds to a constant distribution of equally strong Debye relaxations between some upper (τ_1) and lower (τ_2) limits [24]:

$$g(\tau) = \begin{cases} \dfrac{\Delta\varepsilon}{\ln a} = B & \tau_2 \leqslant \tau \leqslant \tau_1 \\ 0 & \tau < \tau_2,\ \tau > \tau_1 \end{cases} \tag{6}$$

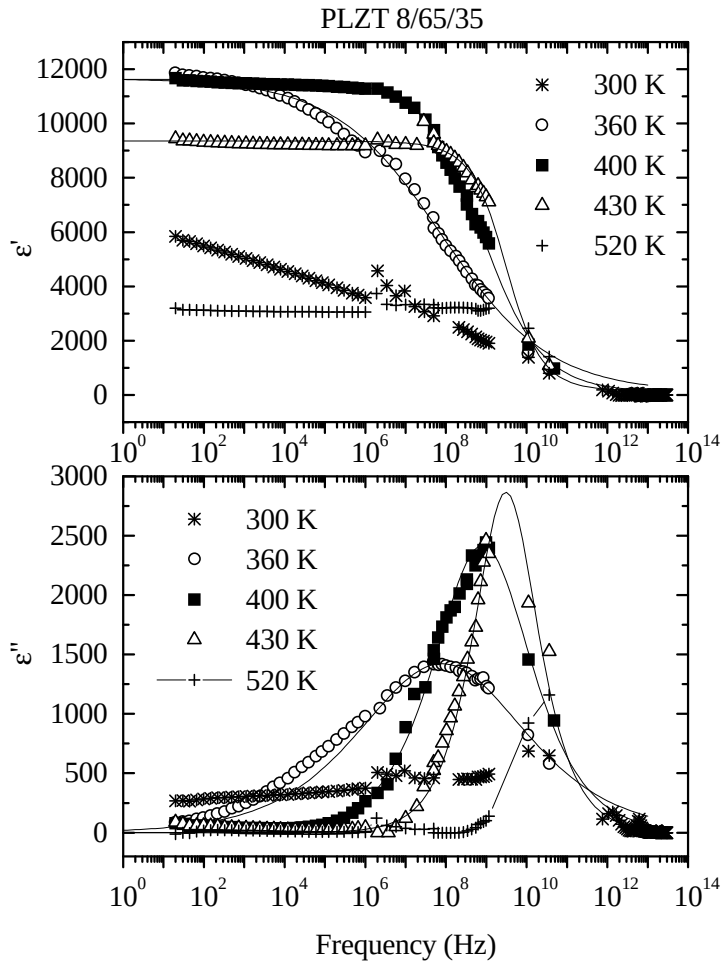

Figure 4. Frequency dependence of real and imaginary part of the complex permittivity of PLZT 8/65/35 at various temperatures. The continuous curves are Cole–Cole fits with the parameters shown in figure 9; points are experiment. Points above 10^{12} Hz are taken from the fit of room-temperature IR spectra.

where B is independent of τ and

$$a = \tau_1/\tau_2 \tag{7}$$

is a parameter of the uniform distribution.

Our choice of the uniform $g(\tau)$ for the analysis is justified by the following reasoning. First, uniform $g(\tau)$ is the simplest case and allows us to estimate the width, upper and lower limits of the relaxation time distribution. At the same time, the integral in (4) is not sensitive to the exact shape of the distribution function. Second, it just suits the case of the PLZT dielectric spectra: high level of broadening, very wide distribution of the relaxation times, symmetrical shape of the Cole–Cole plots. Third, parameters of the uniform distribution can be easily defined from the Cole–Cole equation parameters [24], because both uniform $g(\tau)$ and Cole–Cole equation correspond to the symmetrical distribution of relaxation times in the logarithmic scale. The uniform $g(\tau)$ was also used for analysis of the dielectric spectra of

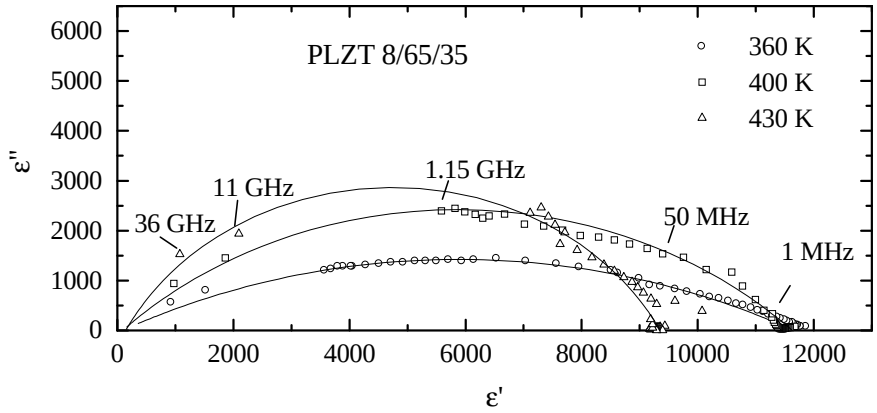

Figure 5. Cole–Cole plots of PLZT 8/65/35 for different temperatures. The continuous curves are fits with the Cole–Cole model.

the best investigated relaxor PMN (lead magnesium niobate) and the best investigated dipolar glass $Rb_{2-x}(NH_4)_xD_2PO_4$ [26–29].

In the case of uniform $g(\tau)$, equation (4) results in the following expressions for the real and imaginary parts of the dielectric permittivity [24]:

$$\varepsilon'(\omega) = \varepsilon_\infty + \frac{B}{2}\ln\left(\frac{a^2+\omega^2\tau_1^2}{1+\omega^2\tau_1^2}\right) \tag{8}$$

$$\varepsilon''(\omega) = B\,\tan^{-1}\left[\frac{\omega\tau_1(a-1)}{\omega^2\tau_1^2+a}\right]. \tag{9}$$

The maximal value of the dielectric loss depends on the distribution parameter a and decreases with increasing a:

$$\varepsilon''_{\max}(\omega) = B\,\tan^{-1}\left(\frac{a-1}{2\sqrt{a}}\right). \tag{10}$$

The maximal value of the dielectric loss can be also defined from the Cole–Cole equation (3). It depends on the distribution parameter α [24]:

$$\varepsilon''_{\max} = \frac{\Delta\varepsilon}{2}\cos\left(\frac{\pi\alpha}{2}\right)\left[1+\sin\left(\frac{\pi\alpha}{2}\right)\right]^{-1}. \tag{11}$$

Comparison of the equations (10) and (11) allows to calculate the parameter a from the known parameter α. Temperature dependences of a, calculated from the $\alpha(T)$ dependences in figure 9, are shown in figure 10. As expected, one can see that the distribution width increases critically with decreasing temperature, achieving extremely high values (about 11 decades for PLZT 9.5/65/35 at 300 K). $a(T)$ dependences can be well fitted to the Vogel–Fulcher-like law:

$$a(T) = a_0\exp\left(\frac{U}{T-T_{VF}}\right) \tag{12}$$

with the same critical temperature $T_{VF} = 230$ K for both (!) investigated PLZT ceramics. a_0 and U are temperature independent constants.

Characteristic times τ_1 and τ_2 of the uniform distribution are related to the mean relaxation time τ_0 of the Cole–Cole equation:

$$\ln\tau_0 = \frac{\ln\tau_1 + \ln\tau_2}{2}. \tag{13}$$

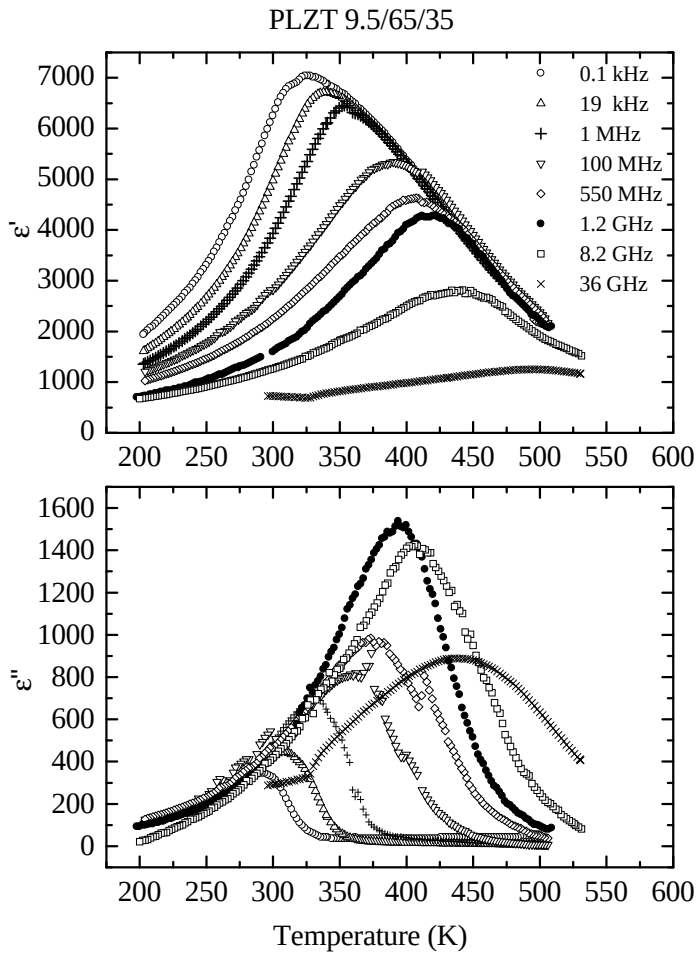

Figure 6. Temperature dependence of real (ε') and imaginary (ε'') part of complex permittivity of PLZT 9.5/65/35 ceramics at various frequencies.

Solving the system of equations (7) and (13), one can find the upper (τ_1) and lower (τ_2) limits of distribution of relaxation times. So, combination of the Cole–Cole equation and the uniform $g(\tau)$ allows us to estimate the mean relaxation time as well as the limits of distribution of relaxation times. Figure 11 shows temperature dependences of τ_1 and τ_2, calculated from the parameters τ_0 and a in figures 9 and 10.

The upper time τ_1 increases with decreasing temperature like τ_0 but much faster (about 10^7 times in the interval of 100 K for PLZT 9.5/65/35), while τ_2 is almost temperature independent with a value about 10^{-11} s to 10^{-12} s. Temperature dependences of both τ_1 and τ_0 do not obey properly the Arrhenius law. Therefore we have fitted them with the Vogel–Fulcher law, usually used for relaxor ferroelectrics and glassy systems [27, 28]:

$$\tau(T) = \tau_L \exp\left(\frac{U_{VF}}{T - T_{VF}}\right) \tag{14}$$

where T_{VF} is the Vogel–Fulcher freezing temperature where the relaxation time diverges, U_{VF} is the activation energy and τ_L is the limiting high-temperature relaxation time which should

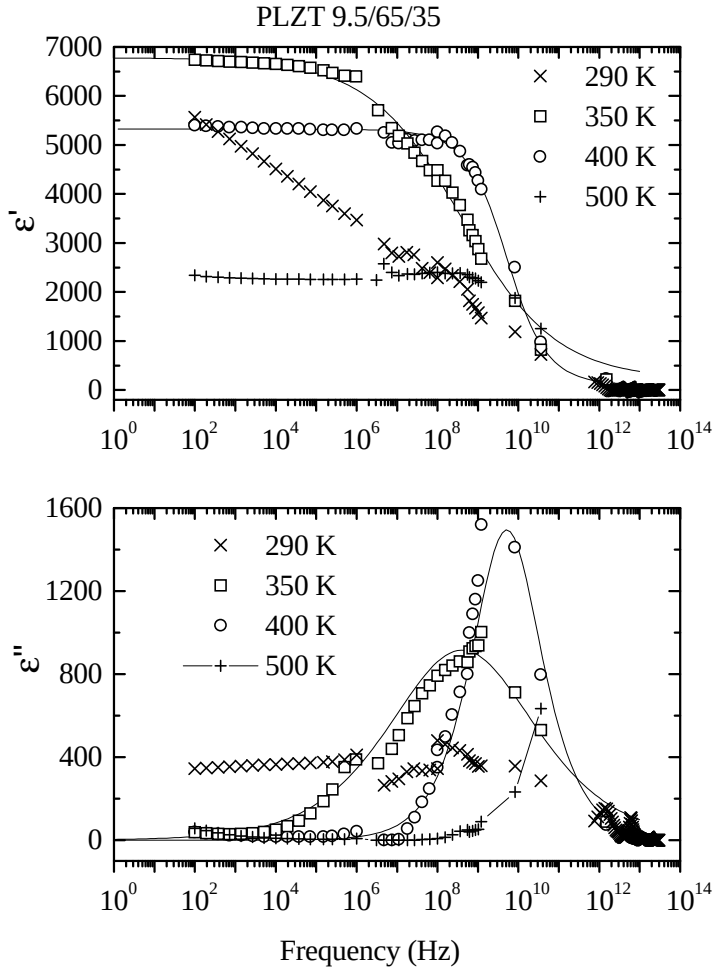

Figure 7. Frequency dependence of permittivity (ε') and losses (ε'') of PLZT 9.5/65/35 ceramics at various temperatures. The continuous curves are fits with the parameters shown in figure 9; points are experiment. Points above 10^{12} Hz are taken from room-temperature IR spectra.

be of the order of the reciprocal lowest optic phonon frequency. Solid and dashed lines in figure 11 are the fits. Both τ_1 and τ_0 fit well to the Vogel–Fulcher law with the same critical freezing temperature $T_{VF} = 230$ K $\pm$ 5 K. The same value of T_{VF} for τ_1 and τ_0 (as well as for the distribution parameter a) can be understood taking into account that τ_2 is nearly temperature independent.

The mean relaxation time fit results in the values of $\tau_L = (5.8 \pm 0.5) \times 10^{-14}$ s for PLZT 8/65/35 and $\tau_L = (6.6 \pm 0.5) \times 10^{-14}$ s for PLZT 9.5/65/35, corresponding to the vibration frequencies of 91 and 80 cm^{-1} respectively, quite close to the lowest polar phonon frequencies (75 cm^{-1} at 10 K, see table 2). The activation energies were estimated as $U_{VF}[\tau_0] = 1370$ K $\pm$ 50 K, $U_{VF}[\tau_1] = 2900$ K $\pm$ 100 K for PLZT 8/65/35 and $U_{VF}[\tau_0] = 1040$ K $\pm$ 30 K, $U_{VF}[\tau_1] = 2220$ K $\pm$ 100 K for PLZT 9.5/65/35. While the activation barriers are smaller for higher La concentration, surprisingly the same value of T_{VF} was obtained for both studied ceramics.

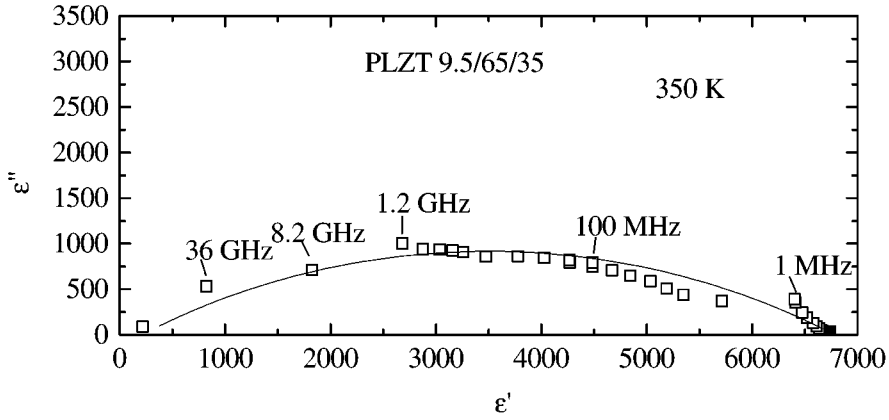

Figure 8. Cole–Cole plot of PLZT 9.5/65/35 ceramics.

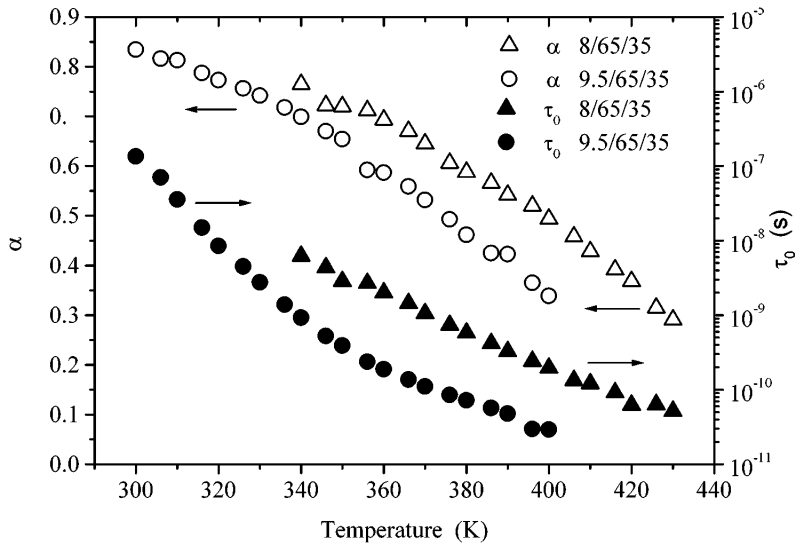

Figure 9. Temperature dependences of the Cole–Cole equation parameters.

3.4. Analysis of the low-temperature dielectric spectra of PLZT 9.5/65/35

The low-temperature dielectric spectra were analysed on the basis of uniform $g(\tau)$, analogously to the approach recently used by Cheng *et al* for PMN [26]. At low enough temperatures we can assume that $\omega\tau_1 \gg 1$ and $\omega\tau_2 \ll 1$, i.e. our data correspond to the frequency range of $1/\tau_1 \ll \omega \ll 1/\tau_2$, where our measurement frequency range is much narrower than the range of relaxation frequencies. This assumption is valid below the freezing temperature, as well as in the some interval above it, because τ_1 becomes extremely high already at $(T - T_{VF}) \approx 70$ K (see figure 11). Taking into account that the value of $1/\tau_2$ is only a few orders of magnitude lower than the optical phonon frequencies, this assumption is valid at least at frequencies below 1 MHz. Then the equations (8) and (9) can be written as:

$$\varepsilon'(\omega) = \varepsilon_\infty - B(T)\ln(\omega\tau_2) \tag{15}$$

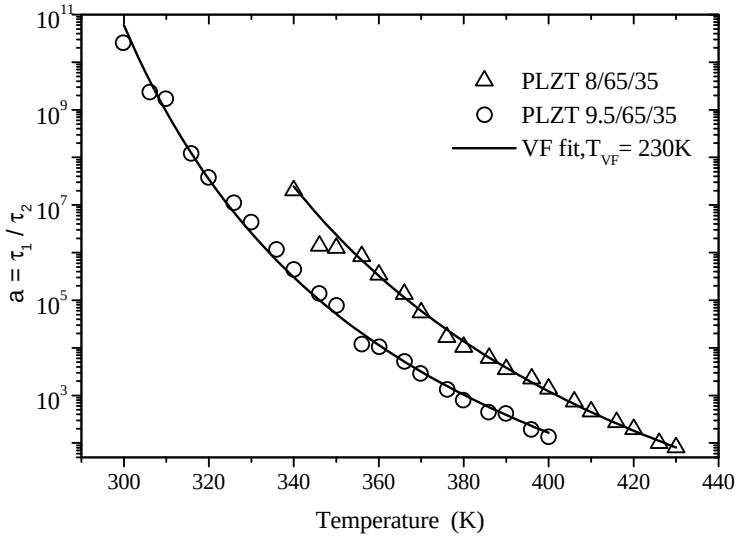

Figure 10. Temperature variations of the uniform distribution parameter a.

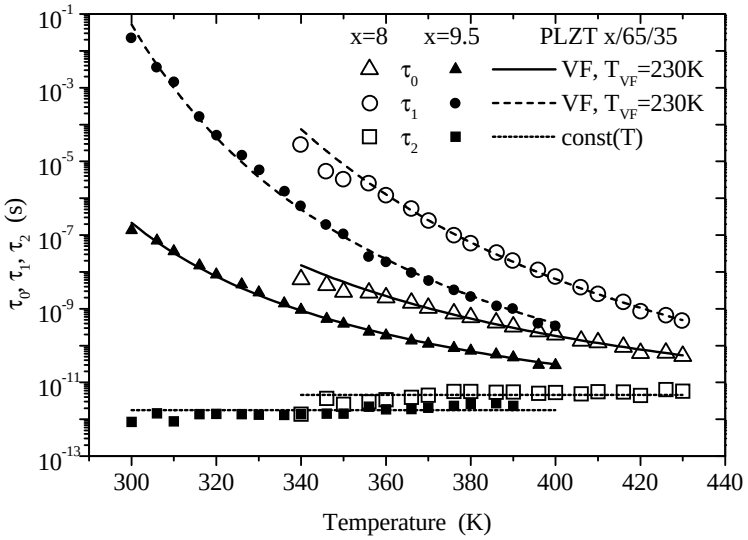

Figure 11. Temperature variation of the mean, upper and lower relaxation times, estimated from the uniform distribution model.

$$\varepsilon''(\omega) = \frac{\pi}{2} B(T) \tag{16}$$

where $B(T)$ is the frequency independent but temperature dependent parameter introduced in (6).

According to this model, at low temperatures and in some limited but broad frequency region, dielectric permittivity should linearly increase with decreasing frequency on a logarithmic scale, while dielectric loss should be independent of frequency. Our experimental data fit well to the equations (15) and (16) at temperatures below 290 K (figure 12). Dielectric

loss spectra are nearly frequency independent in the range from 100 Hz to 1 MHz, at higher frequencies they increase and the maximum is observed at 10^8–10^9 Hz (the scatter of the experimental points above 1 MHz in figure 12 is explained by joining the results of different methods, using several samples of different geometry). Analysing the deviation of the experimental data from this dependence, we can see that the freezing temperature must be lower than 270 K. At higher temperatures, the frequency dependence of ε'' becomes pronounced, indicating the $T > T_{VF}$ regime. This is in agreement with our estimate of T_{VF} from the high-temperature data.

The temperature dependence of the fitting parameter $B(T)$ is shown in figure 13. The decrease in $B(T)$ with the temperature decrease corresponds to the change of the slope of $\varepsilon'(\omega)$ dependences in figure 12. The $B(T)$ dependence can be well fitted with the power law

$$B(T) = cT^d \tag{17}$$

with $c = (3.15 \pm 1.44) \times 10^{-8}$ and the exponent $d = 4.04 \pm 0.07$. For further discussion, the quantity $B(T)$ defined in equation (6) has been plotted also at temperatures above 300 K.

4. Discussion

Let us first discuss our IR spectra. The previously published reflectivity data in a more restricted temperature range [16, 30, 31] agree within the limits of measurement accuracy with our spectra. Neglecting the fact that PLZT is a solid solution rather than a pure stoichiometric compound, three IR active phonon modes of F_{1u} symmetry are expected in the ideal cubic paraelectric phase. However, our careful fit of reflectivity with generalized oscillator formula (equations (1) and (2)) revealed six phonon modes between 530 and 300 K. The activation of additional three weak modes is probably caused by local symmetry breaking due to the formation of polar dynamic nanoclusters with rhombohedral symmetry [7] below the Burns temperature ($T_B \cong 620$ K). This assignment is supported by the fact that the weak modes are more pronounced at low temperatures where the density and dipole moment of clusters become higher. Factor group analysis in rhombohedral phase with the space group $R3c$ ($Z = 2$) gives the following optical modes [17]

$$\Gamma_v = 4\mathrm{A}_1(z, x^2 + y^2, z^2) + 9\mathrm{E}(x, y, x^2 - y^2, xy, xz, yz) + 5\mathrm{A}_2(-).$$

This means that five A_2 modes are silent in IR and Raman spectra while four A_1 and nine E modes are both IR and Raman active. Not all phonon modes are resolved in our spectra, apparently due to their low intensities and/or high damping. Only seven modes are seen in the spectra at 10 K (see figure 1 and table 2).

Similar conclusions about the broken symmetry in the paraelectric phase and disorder down to low temperatures follow also from the published Raman spectra [30, 10–12, 17]. The differences between Raman and IR mode frequencies can be understood as a consequence of the cluster anisotropy, as discussed in [17].

Concerning the softening of our lowest-frequency mode towards T_B, it is natural to suggest that this mode represents the local ferroelectric soft mode within each polar cluster. If this assignment is correct, one would expect hardening of this mode above T_B. Moreover, as is seen from figures 4, 7 and 11, the MW dispersion approaches the soft-mode response on heating towards T_B. Obviously, the MW dispersion close to T_B is due to the cluster dipole flipping which should vanish above T_B. Hence, above T_B the whole MW and submillimetre response should reduce into one overdamped phonon mode which hardens on further heating. To check these features, additional high-temperature submillimetre and MW measurements are of great interest.

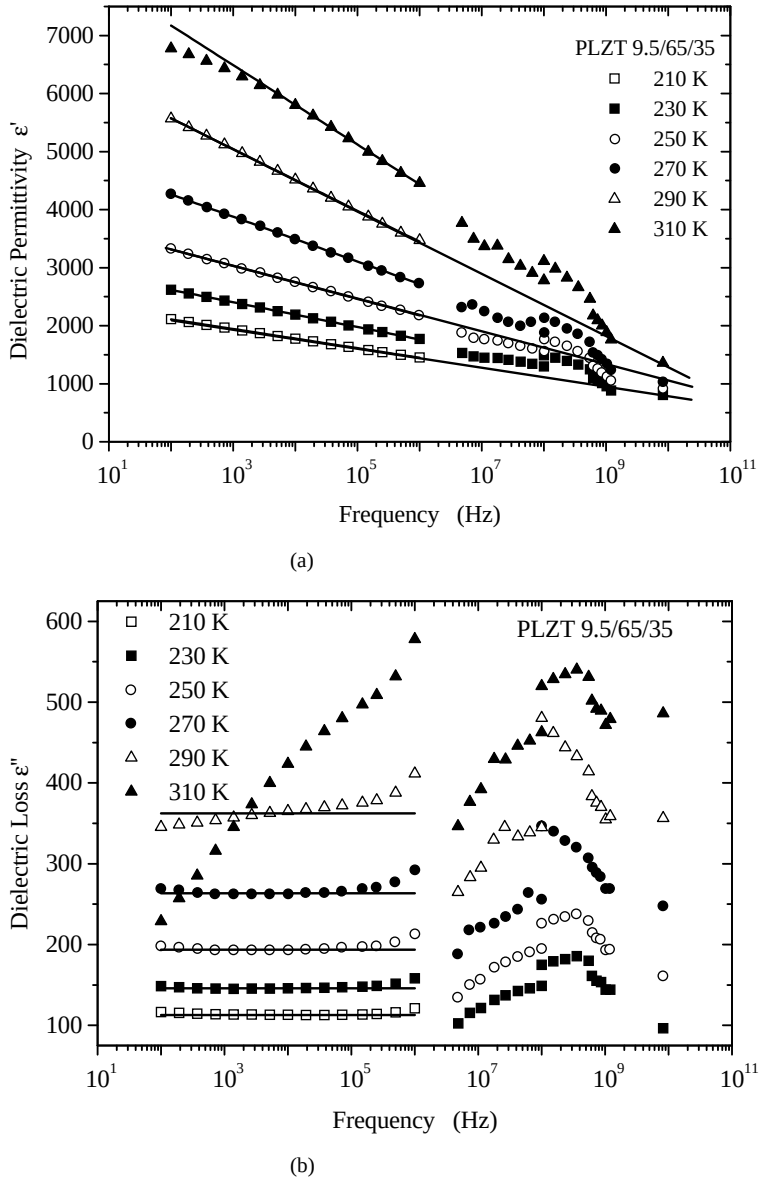

Figure 12. Frequency dependences of the complex dielectric permittivity of PLZT 9.5/65/35 at various temperatures. Points are experimental, solid lines represent the simultaneous fit with equations (15) and (16), respectively. (a) Real part (ε'); (b) imaginary part (ε'').

Let us now disscuss the MW and lower-frequency dielectric data. At elevated temperatures (near and above T_m: i.e. above 340 K for PLZT 8/65/35 and above 300 K for PLZT 9.5/65/35) only one dominant dispersion mechanism below phonon frequencies contributes to the broad-frequency-range dielectric response. The properties of this dielectric dispersion completely contradict the results of [9] and [10], but are in agreement with the most recent data in [15].

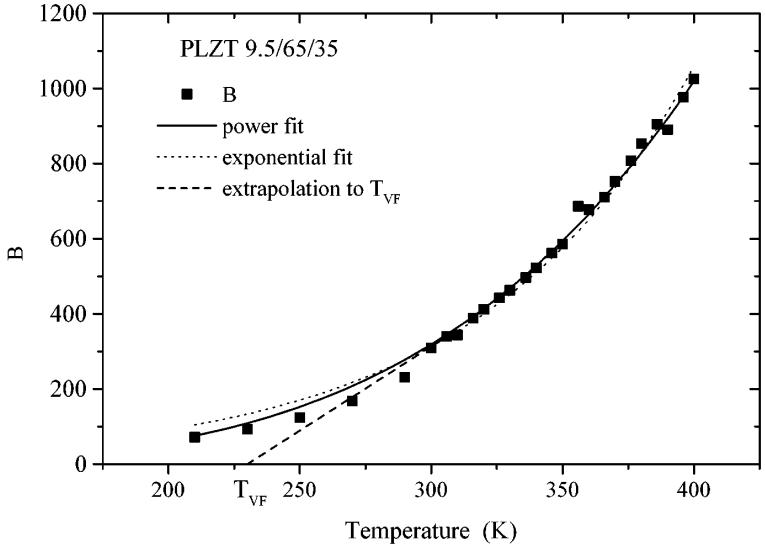

Figure 13. Temperature dependence of the parameter B.

Our results can be understood within the model of Cheng *et al* [26, 27], who also used uniform $g(\tau)$ for the simulation of dielectric response of the relaxor ferroelectric PMN. According to their model, the distribution of the relaxation times in the relaxor phase is determined by the size distribution of the polar regions and should be dependent on temperature. The lower limit τ_2 is associated with the smallest polar regions having the volume of a crystalline unit cell, it is temperature independent and equal to τ_L. The upper limit τ_1 is associated with the largest polar regions; it is strongly dependent on the temperature as the mean volume of polar regions increases with decreasing temperature and the interactions among them cause the freezing of the local dipole moments when approaching the freezing temperature [32]. Besides the dipole reversal of the polar regions, the fluctuations of their amplitudes and the dipole fluctuations inside the space among the polar regions are assumed to contribute to the dielectric response. The last mechanism is the leading contribution at lower temperatures (and at higher frequencies) when the reversal of the polar regions process is effectively frozen out, and it is mainly realized as the fluctuations of the polar region boundaries [33].

Unlike in the model of Cheng *et al* [26, 27], for the description of temperature dependences of τ_1 and τ_0 in the relaxor phase we prefer to use the Vogel–Fulcher law as a more physically justified one [32] rather than the super-exponential function [27]. Also, we made no *ad hoc* assumption about the value and temperature dependence (or independence) of τ_2. Nevertheless, we obtained that τ_2 is almost temperature independent and we can fit it acceptably also with the Arrhenius law that is consistent with the thermal reversal of the smallest polar regions. Assuming the same $\tau_L = 6 \times 10^{-14}$ s the fitted energy barrier is $U_A = 1080 \pm 50$ K. The value of τ_2 differs from the value of τ_L by less than 100-fold (the τ_2/τ_L ratio is about 80 for PLZT 8/65/35 and 30 for PLZT 9.5/65/35). This indicates that the volume of the smallest polar regions is nearly temperature independent, but somewhat bigger than the volume of a unit cell. If we assume that τ_2 increases with the volume of the smallest polar region, higher τ_2/τ_L ratio for the PLZT 8/65/35 than 9.5/65/35 could be related to the bigger volume of these regions in the former case. This correlates with the increase in the polar region concentration (or volume fraction) with the decrease in La content, which might be naturally expected taking

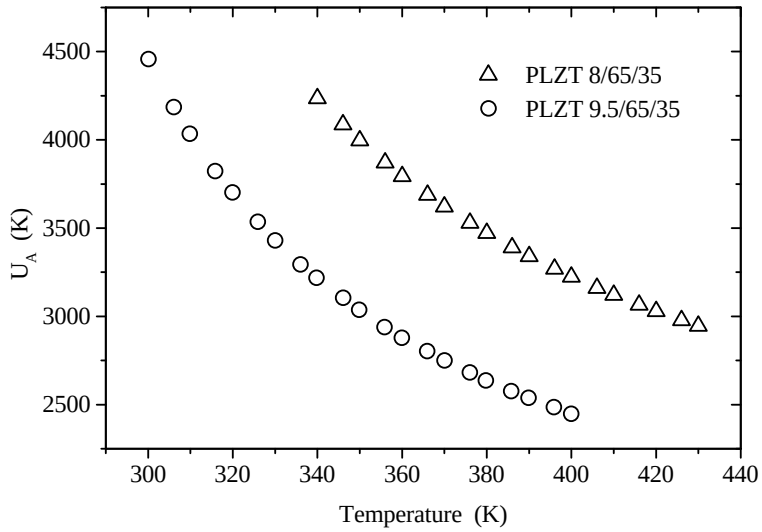

Figure 14. Temperature dependence of the activation energy.

into account that for less than ∼4 at.% of La macroscopic ferroelectric domains appear and even for 6–7 at.% of La a spontaneous transition into ferroelectric phase slowly occurs [34].

The ratio between the upper limit and the mean activation energies $U_{VF}[\tau_2]/U_{VF}[\tau_0] \approx 2$ is the same for both PLZT ceramics. This value could be understood taking into account that the distribution of relaxation times is a consequence of the distribution of the potential barriers for individual relaxors. Therefore equation (13) is equivalent to the following definition of the mean activation energy:

$$U_{VF}[\tau_0] = \frac{U_{VF}[\tau_1] + U_{VF}[\tau_2]}{2} \tag{18}$$

where $U_{VF}[\tau_1]$ is defined by the potential barrier for the biggest polar regions and $U_{VF}[\tau_2]$ by the potential barrier for the smallest polar regions. Because the activation energy of a polar region relaxation is assumed to be proportional to its volume [3, 26], $U_{VF}[\tau_1] \gg U_{VF}[\tau_2]$ and in the case of nearly temperature independent τ_2, $U_{VF}[\tau_2] \approx 0$. Therefore $U_{VF}[\tau_1]/U_{VF}[\tau_0] \approx 2$. The distribution of the heights of potential barriers at temperatures far above T_{VF} is in the interval from ≈0 K to ≈3000 K for PLZT 8/35/65 and from ≈0 K to ≈3000 K for PLZT 9.5/35/65.

The U_{VF} corresponds to the height of the potential barrier of the relaxator (and consequently it has the meaning of 'true' activation energy U_A) only at temperatures far above T_{VF}. We may consider that the Vogel–Fulcher law (14) reflects the increase in the 'true' activation energy with the temperature decrease and is equivalent to the Arrhenius equation with a temperature dependent activation energy $U_A(T)$:

$$\tau(T) = \tau_L \exp\left[\frac{U_A(T)}{kT}\right]. \tag{19}$$

Comparison of equations (14) and (19) results in the temperature dependence of the mean activation energy which tends to diverge at T_{VF} (see figure 14). The increase in U_A with decreasing temperature can be understood by the increase in the size and the dipole moment of polar regions which have to be switched and in increase in interactions among them.

Within the framework of the theory of universal dielectric response [35] the dielectric spectrum follows the power laws $\chi''(\omega) \propto \omega^m$ and $\chi''(\omega) \propto \omega^{1-n}$, below and above the loss maximum, respectively. In the relaxor phase the symmetric Cole–Cole equation (3) gives $m = 1 - n = 1 - \alpha$, $0 < m, n < 1$. In the low-temperature phase the flat loss spectrum can be described with $m \approx 0$ and $n \approx 1$. The exponents m and n were given a particular physical meaning [35]. Above the maximum of the spectrum, $n \approx 1$ means that the response is contributed mainly by the field induced dynamical clusters that possess strong intracluster correlations, i.e. each cluster preserves its coherence during the motion (in contrast to this, the clusters consisting of independent dipoles would result in Debye relaxation, $n = 0$). At lower frequencies below the loss maximum the spectrum is characterized by $m \approx 0$, and this can be interpreted as a consequence of strong intercluster correlations. Thus the generalized model of Dissado and Hill [35] gives a qualitative mechanism underlying the broadening of relaxation spectra at higher and lower frequencies. The dynamical clusters considered here mean the field induced dynamical displacements correlated within a certain distance and should not be identified with the polar regions frozen out at low temperatures.

From our data it follows that the temperature changes in the relaxation dynamics of PLZT 8/65/35 and 9.5/65/35 are similar, but there is a temperature shift of the slowing down process and at the same time there is no shift of the freezing temperature T_{VF}. Hence we conclude that the difference in relaxation dynamics of both samples is not caused by the shift of the freezing temperature, but by the change of scale of activation energies. This can be understood assuming that the collective freezing process at the temperature T_{VF} is determined by interactions among the polar clusters, while the local activation barriers of the dipole flipping are responsible for the time-scale of the ordering process. Then the small concentration variation of La ions affects the activation barriers only leaving the inter-cluster interactions untouched. A higher concentration difference of La ions should result also in the shift of T_{VF}.

We would like to point out that our T_{VF} differs from that usually evaluated in the literature [5, 11]. Usually, one takes the maxima from the real permittivity or loss–temperature plots at several fixed frequencies and takes them as the characteristic relaxation frequencies at the corresponding temperatures of maxima. It is easy to show [36] that the Vogel–Fulcher temperature from such plots does not necessarily correspond to the divergence of the real relaxation time determined using maxima from the loss–frequency plots. In our way of evaluation, however, the mean relaxation time directly corresponds to the frequency of the loss spectrum maximum. Therefore, a direct comparison of our T_{VF} is possible only with the recent result of the Kutnjak approach [15] which yields $T_{VF} = 249$ K. Taking into account the different source of samples in [15] and the uncertainty in determination of the static permittivity at lower temperatures, which is needed for the Kutnjak approach, the agreement is quite satisfactory.

Let us comment briefly on the relation between our T_{VF} and the freezing temperature T_f. Unlike T_{VF} which has the meaning of extrapolated temperature divergence of the linear dielectric response time (in weak fields), T_f is frequently determined [5, 11] as a temperature where the remanent polarization P_r of the previously poled (in strong fields) sample vanishes. The latter definition has two complicating features. The vanishing of P_r is not sharp and complete and moreover this process is time dependent in the sense that slower heating shifts T_f downwards. Therefore it can be understood that the T_f temperatures found in the literature show an appreciable scatter, but in all cases $T_f > T_{VF}$. Alternatively, T_f may be more precisely defined as the temperature where splitting of the field cooled and zero-field cooled static permittivity occurs ([15] and references therein). But even here the problem remains with the determination of the really static permittivity.

Owing to no change of macroscopic symmetry during the freezing process, the total dielectric strength $\Delta\varepsilon$ should remain finite at and below the freezing temperature T_{VF}. On the other hand, the longest relaxation time τ_1 diverges at T_{VF} and therefore the coefficient $B(T)$ should approach 0 for $T \to T_{VF}$. In contrast to this our data show that $B(T_{VF}) > 0$. This apparent discrepancy can be resolved by realizing how the relaxation time and the parameter $B(T)$ were determined from experiment. Due to the extremely broad spectrum within the freezing region the Vogel–Fulcher temperature T_{VF} is obtained by fitting the data from higher temperatures (above 300 K), and the fitting parameter T_{VF} can be treated as the ideal freezing temperature reflecting the collective nature of the freezing process. At T_{VF} nearly all processes described by the constant distribution of relaxation times with the Vogel–Fulcher upper relaxation time are frozen out and cannot contribute to the permittivity (since $\varepsilon' \to \varepsilon_\infty$ in the limit $\tau_1 \to \infty$, $\omega > 0$). However, dynamic processes also exist that do not freeze in at T_{VF} and contribute to the dielectric response both below and above the freezing temperature. They were not taken into account at higher temperatures. These processes tend to conceal the ideal freezing transition. Then, instead of divergence of the relaxation time obtained as a result of the fitting procedure (and our assumption of the Vogel–Fulcher law) from the higher temperatures, the crossover from the Vogel–Fulcher law above T_{VF} to the Arrhenius law below T_{VF} is expected to appear. This is a common feature of disordered systems observed e.g. in supercooled liquids [37]. Since the value $B(T_{VF}) = (2/\pi)\varepsilon''$ is measured directly around T_{VF} (and not fitted from the high-temperature data) it should display this crossover. In figure 13 the temperature plot of $B(T)$ is shown. The squares represent data from equations (15) and (16) (below 300 K) and from equation (6) (above 300 K). The relaxation time τ_1 was evaluated above room temperature only and afterwards extrapolated to T_{VF} where it diverges. The corresponding extrapolation of $B(T)$ down to T_{VF} from higher temperatures is plotted as the dashed line. Deviation of the dashed line from the real measured points represents the above-mentioned crossover. Let us recall that the constant distribution of relaxation times is considered in this discussion, where the upper-relaxation-time behaviour is different at high and low temperatures. Even if the form of the relaxation time distribution can be actually more complicated (particularly close above T_{VF}), the basic features of the freezing process are expected to be well described within this simple model.

At low temperatures the dielectric spectrum is very broad and evaluation of the upper relaxation time is beyond our experimental frequency range. On the basis of previous discussion below T_{VF} we assume rather the Arrhenius temperature behaviour of the relaxation time $\tau_1 = \tau_L \exp(U_{\max}/kT)$, where $U_{\max}$ is the temperature independent value of the energy barrier which is certainly higher than the maximal value of U_A from figure 14. Note that now the system is effectively in the nonergodic phase and, in contrast to the high-temperature phase, the distribution of relaxation times is attributed mainly to the inter-cluster regions, the polar region reversal processes being frozen out. Then the relation between the static permittivity and the coefficient $B(T)$ can be obtained from its definition (equations (6), (17), (19)):

$$\varepsilon_s(T) \cong \frac{U_{\max}}{kT} B(T) \propto T^{d-1}. \tag{20}$$

In our case it predicts a decrease in the static permittivity with cooling proportionally to T^3 in the temperature range close below T_{VF} (at least 210–230 K). However, this conclusion, which is based on the assumption of the uniform distribution of relaxation times with Arrhenius-type temperature dependence of the mean relaxation time, as well as the actual value of $U_{\max}$, should be verified by reliable very low-frequency dielectric experiment near and below T_{VF}.

In glasses ε'' increases monotonically with increasing temperature and, over a limited temperature range, the temperature dependence of ε'' can obey a power dependence T^α or exponential dependence $\exp(T/T_0)$ [38]. The coefficient $B(T)$ should possess the same

temperature dependence as ε''. Cheng *et al* [27] have fitted the temperature dependence of the parameter $B(T)$ with an exponential formula $B_0 \exp(CT)$. Our similar fit with $B_0 = 8.1 \pm 1.0$ and $C = (1.22 \pm 0.33) \times 10^{-2}$ K^{-1} is shown in figure 13 by a dotted line. We have also used here the power law with an attempt to give a certain physical interpretation to the exponent d. At low temperatures the switchable elementary dipoles (residing mainly in the inter-cluster regions) move around equilibrium positions in potentials of diverse forms due to the presence of disorder. In principle, the free energy expansion $F(P)$ with respect to the polarization P can be carried out. Instead, for the sake of simplicity, we consider $F \propto |P|^n, n > 0$. This term can be understood as an effective potential resulting from the thermal fluctuations of polarization and allowing estimation of its anharmonic character. In the harmonic potential $n = 2$, while n deviates from 2 of the anharmonic terms become important. Using the general theory of dielectric response, the static susceptibility corresponding to the above effective potential is

$$\chi(0) = \langle P^2 \rangle / kT \propto (kT)^{\frac{2}{n}-1}. \tag{21}$$

Finally, taking into account $\varepsilon_s \gg \varepsilon_\infty$, and $\varepsilon_s = \varepsilon_v \chi(0) + 1$ (ε_v is the permittivity of vacuum), the coefficient $B(T)$ reads:

$$B(T) = \frac{\varepsilon_s - \varepsilon_\infty}{\ln(\tau_1/\tau_L)} \propto T^{2/n}. \tag{22}$$

The exponent n indicates the form of the average potential that is inspected by the polarization: $n = 2$ corresponds to a harmonic potential, i.e. temperature independent response. For $n > 2$ (flat bottom) the susceptibility increases with cooling (note that according to the Landau theory $n = 4$ at the transition point) and for $n < 2$ the susceptibility decreases with cooling. Comparing equations (17) and (22) the exponent is $n = 2/d$ and from our fit $n \cong 1/2$. This represents a nonlinear potential for the polarization fluctuations in the considered temperature range. The exponent n should depend on the temperature and at temperatures near zero it is expected to approach the higher value $n \approx 2$ corresponding to the harmonic potential of vibration modes.

The above approach describes well the decrease in the losses and the slope of the $\varepsilon' - \ln \omega$ dependence with cooling at least above 20 Hz. On the other hand we stress again that the lowest limiting relaxation frequency, the static permittivity and their temperature dependences discussed above have not yet been experimentally investigated. Therefore the low-frequency studies near and below T_{VF} are of great interest. However, we recall that below the freezing point the system is non-ergodic and its behaviour depends on the pre-history. Our results have been obtained under slow cooling runs from the highest temperatures without bias field. Another interesting point could be e.g. the studies of dielectric properties on cooling under bias fields of various magnitudes or on heating. Also the speed of the temperature changes and sample aging may play a role.

5. Conclusions

For the first time the complete dielectric dispersion of a relaxor ferroelectric was studied in a broad temperature and frequency interval including the MW and IR range and low temperatures below the freezing point. Two materials with a very high permittivity frequently used for applications, namely PLZT 8/65/35 and 9.5/65/35, were investigated. The IR spectra indicate the presence of polar nanoclusters in the whole temperature range 10–530 K. A softening of the lowest polar mode was observed with the extrapolated softening temperature close to the Burns temperature $T_B \cong 620$ K where the clusters begin to appear on cooling. Below T_B additional strong MW dispersion appears which is assigned to flipping of the clusters. On

cooling the dispersion and loss spectra strongly broaden and slow down, but remain symmetric so that the Cole–Cole model is applicable. This enabled us to determine also the width of the uniform distribution function of the relaxation times and its temperature dependence above room temperature. The longest and mean relaxation times diverge according to the Vogel–Fulcher law with the same freezing temperature $T_{VF} \cong 230$ K for both materials. The shortest relaxation time is about 10^{-12} s and remains almost temperature independent. The only remarkable difference between both materials is an appreciably higher Vogel–Fulcher activation energy in the case of PLZT 8/65/35 which causes faster broadening of the spectra on cooling and higher low-frequency permittivity values. The spectra are compatible with the Jonscher's universal law and the broadening indicates a strong increase in inter-cluster correlation. Below room temperature the spectra become so broad that the low-frequency cut-off is much below 20 Hz (our lowest measured frequency) and the losses become independent of frequency. Appreciably high and temperature dependent losses and permittivity dispersion were observed also below T_{VF} in the nonergodic frozen phase. The quantitative estimates indicate a strongly anharmonic potential for polarization fluctuations which are restricted to inter-cluster boundaries.

Acknowledgments

The work was supported by the Grant Agency of the Czech Republic (project No 202/98/1282) and the Grant Agency of the Academy of Science of the Czech Republic (project No A1010828).

References

[1] Haertling G H 1987 *Ferroelectrics* **75** 25
[2] Cross L E 1994 *Ferroelectrics* **151** 305
[3] Viehland D, Jang S J, Wuttig M and Cross L E 1990 *J. Appl. Phys.* **68** 2916
Viehland D, Jang S J, Wuttig M and Cross L E 1991 *J. Appl. Phys.* **69** 6595
[4] Darlington C N W 1989 *Phys. Status Solidi* a **113** 63
[5] Viehland D, Li J F, Jang S J, Cross L E and Wuttig M 1992 *Phys. Rev.* B **46** 8013
[6] Burns G and Dacol F H 1983 *Phys. Rev.* B **28** 2527
[7] Viehland D, Xu Z and Payne D A 1993 *J. Appl. Phys.* **74** 7454
[8] Kersten O, Rost A and Schmidt G 1983 *Phys. Status Solidi* a **75** 495
[9] Schmidt H and Dörr A 1989 *Ferroelectrics* **93** 309
[10] Dellis J-L, Dalleunes J, Carpentier J-L, Morell A and Farhi R 1994 *J. Phys.: Condens. Matter* **6** 5161
[11] Farhi R, El Marsi M, Dellis J-L, Picot J-C and Morell A 1989 *Ferroelectrics* **176** 99
[12] Dellis J-L, El Marsi M, Tilloloy P, Farhi R and Viehland D 1997 *Ferroelectrics* **201** 167
[13] Dimza V I 1996 *J. Phys.: Condens. Matter* **8** 2887
[14] Tan Q and Viehland D 1998 *Ferroelectrics* **209** 582
[15] Kutnjak Z, Filipic C, Pirc R, Levstik A, Fahri R and El Marssi M 1999 *Phys. Rev.* B **59** 294
[16] Zelezny V, Petzelt J, Volkov A A and Ozolinsh M 1990 *Ferroelectrics* **109** 149
[17] Pokorny J, Petzelt J, Gregora I, Zelezny V, Vorlicek V, Zikmund Z, Fedorov I, Pronin A and Kosec M 1996 *Ferroelectrics* **186** 115
[18] Fedorov I, Petzelt J, Zelezny V, Volkov AA, Kosec M and Delalut U 1997 *J. Phys.: Condens. Matter* **9** 5205
[19] Williamson W, Chen H D, Cross L E and Gilbert B K 1997 *Integrated Ferroelectr.* **17** 197
[20] Kamba S, Petzelt J, Banys J, Mizaras R, Grigas J, Pokorny J, Endal J, Brilingas A, Komandin G, Pronin A and Kosec M *Ferroelectrics* **223** 247
[21] Mizaras R, Kajokas A, Banys J, Brilingas A, Grigas J, Kamba S and Petzelt J 1998 *Lith. J. Phys.* **38** 18
[22] Grigas J 1996 *Microwave Dielectric Spectroscopy of Ferroelectrics and Related Materials* (Amsterdam: Gordon and Breach)
[23] Gervais F 1983 *Infrared and Millimeter Waves* vol 8, ed K J Button (New York: Academic) p 279
[24] Poplavko Y M 1980 *Physics of Dielectrics* (Kiev: Vyscha Shkola) (in Russian)

[25] Jonscher A K 1983 *Dielectric Relaxation in Solids* (London: Chelsea Dielectric)
[26] Cheng Z-Y, Katiyar R S, Yao X and Guo A S 1997 *Phys. Rev.* B **55** 8165
[27] Cheng Z-Y, Katiyar R S, Yao X and Bhalla A S 1998 *Phys. Rev.* B **57** 8166
[28] Levstik A, Kutnjak Z, Filipic C and Pirc R 1998 *Phys. Rev.* B **57** 11 204
[29] Kutnjak Z, Filipic C, Levstik A and Pirc R 1993 *Phys. Rev. Lett.* **70** 4015
[30] Lurio A and Burns G 1974 *J. Appl. Phys.* **45** 1986
[31] Nikolic P M, Stojanovic B D, Duric S, Radovic D V, Siapkas D and Zorba T T 1997 *J. Mater. Sci.* **32** 6371
[32] Glinchuk M D and Stephanovich V A 1998 *J. Korean Phys. Soc.* **32** S1100
[33] Tagantsev A K and Glazounov A E 1998 *Phys. Rev.* B **57** 18
[34] Krumins A, Shiosaki T and Koizumi S 1994 *Japan. J. Appl. Phys.* **33** 4940
[35] Dissado L A and Hill R M 1983 *Proc. R. Soc.* A **390** 131
[36] Tagantsev A K 1994 *Phys. Rev. Lett.* **72** 1100
[37] Götze W and Sjögren L 1992 *Rep. Prog. Phys.* **55** 241
[38] Ngai K L 1999 *J. Chem. Phys.* **110** 10 576